Available online at www.sciencedirect.com
ScienceDirect
International Journal of Mass Spectrometry 263 (2007) 1–11
International Journal of Mass Spectrometry
www.elsevier.com/locate/ijms

Development of a PTR-TOFMS instrument for real-time measurements of volatile organic compounds in air

Hiroshi Tanimoto [a,b,*], Nobuyuki Aoki [a,1], Satoshi Inomata [a], Jun Hirokawa [c], Yasuhiro Sadanaga [a,2]

[a] *Atmospheric Environment Division, National Institute for Environmental Studies, 16-2 Onogawa, Tsukuba, Ibaraki 305-8506, Japan*
[b] *Asian Environment Research Group, National Institute for Environmental Studies, Tsukuba, Ibaraki 305-8506, Japan*
[c] *Faculty of Environmental Earth Science, Hokkaido University, Kita 10 Nishi 5, Sapporo, Hokkaido 060-0810, Japan*

Received 14 December 2006; received in revised form 10 January 2007; accepted 10 January 2007
Available online 20 January 2007

Abstract

A proton transfer reaction-time-of-flight mass spectrometer (PTR-TOFMS) has been developed for real-time measurements of volatile organic compounds in air. The instrument is designed to be operated with a hollow cathode discharge ion source and an ion drift tube at relatively high pressures. Each component of the system, an ion source, a drift tube, an ion transfer region, and a time-of-flight mass spectrometer, are in detail characterized by a number of laboratory experiments. The optimized instrumental configuration enables us to gain high intensities of hydronium (H_3O^+) ions, typically $\sim 7 \times 10^5$ counts for 1-min integration at a drift tube pressure of ∼5 Torr. It also suppresses background signals, and interferences from sample air (NO^+ and O_2^+), which undergo fast reactions with volatile organic compounds, to ∼0.5% of those of H_3O^+ ions. We find that the use of the custom-built discharge source show higher overall sensitivities than of a commercially available radioactive source. Potentials to detect oxygenated VOCs (aldehydes, ketones, and alcohols), halocarbons, and amines are also suggested. The detection limits for acetaldehyde, acetone, isoprene, benzene, toluene, and *p*-xylene were determined to be at the sub-ppbv levels for a 1-min integration time. A good linear response at trace levels is certified, but slight sensitivity dependency on water vapor contents is revealed. We finally demonstrate that the instrument can be used for on-line monitoring to detect large variations from emission sources in real-time.

Keywords: Proton transfer reaction; Time-of-flight mass spectrometry; Volatile organic compound; Chemical ionization; PTR-MS

1. Introduction

Volatile organic compounds (VOCs) are a generic name of the compounds that are readily vaporized into the atmosphere at normal temperature and pressure. It is well known that VOCs are emitted from a variety of sources into the atmosphere, and play important roles in controlling air quality by acting as a fuel for gas-phase photochemistry, leading to the formation of ozone and secondary aerosols [1,2]. However, there exist hundreds of VOCs, in particular, around urban area where VOC emissions from human and industrial activities are diverse and strong [3], prohibiting accurate and precise evaluations of the roles of VOCs in air quality issues. It is also widely known that overwhelming amounts of VOCs are emitted from the biosphere including land ecosystems and the ocean into the atmosphere [4,5]. Majorities of biogenically emitted VOCs are short-lived due to their high reactivity, and play a part in not only photochemistry but also in the carbon cycle of the earth [6]. For both anthropogenic and biogenic VOCs, unsaturated (alkene, diene), oxygenated (aldehyde, ketone, alcohol), and aromatic hydrocarbons are recently highlighted in several field studies [7–11]. Owing to a variety of speciation and high reactivity (hence short lifetime and low abundance in air), understanding of the behavior and the roles

* Corresponding author. Tel.: +81 29 850 2930; fax: +81 29 850 2579.
E-mail addresses: tanimoto@nies.go.jp (H. Tanimoto), aoki-nobu@aist.go.jp (N. Aoki), ino@nies.go.jp (S. Inomata), hirokawa@ees.hokudai.ac.jp (J. Hirokawa), sadanaga@chem.osakafu-u.ac.jp (Y. Sadanaga).
[1] Present address: National Metrology Institute of Japan, National Institute of Advanced Industrial Science and Technology, 1-1-1 Umezono, Tsukuba, Ibaraki 305-8563, Japan.
[2] Present address: Department of Applied Chemistry, Osaka Prefecture University, 1-1 Gakuen-cho, Sakai, Osaka 599-8531, Japan.

1387-3806/$ – see front matter © 2007 Elsevier B.V. All rights reserved.
doi:10.1016/j.ijms.2007.01.009

of these VOCs in the atmosphere is still limited by quantity and quality of the measurements, and requires advancement in measurement technologies.

A gas chromatographic (GC) method has been widely used for identification and quantification of VOCs, often being coupled with a mass spectrometer (MS) and/or a flame ionization detector (FID). Although a so-called GC/MS technique has an advantage of separating a number of VOC species and of detecting trace amounts, it commonly suffers from time-resolution. The GC/MS method needs pre-treatment including pre-concentration with cryogenic traps followed by thermal desorption of target species. Also, when air is sampled with canisters or adsorbents, the analysis is off-line and requires further time. Thus analysis with GC/MS is time consuming, and typically takes at least tens of minutes per sample [12]. Also, during sample storage and pre-treatment, species with high reactivity are subject to possible loss and/or transformation by uptake onto metal-surface and by reactions with oxidants (e.g., ozone), respectively [12].

Proton transfer reaction-mass spectrometry (PTR-MS) is a newly developed on-line method that might compliment the conventional GC technique. The proton transfer reaction (PTR) ionization is one of chemical ionization (CI), which enables soft ionization of chemical species that have a proton affinity higher than that of the reagent species (i.e., water in many cases). The PTR from hydronium ions (H_3O^+) occur with many VOCs except low-molecular weight non-methane hydrocarbons (NMHCs), and it produces predominantly protonated ions with less fragmentation than electron-impact ionization (El) does. The PTR-MS instrument was first reported by the group at Innsbruck University [13,14] who coupled a hollow cathode discharge ion source and a drift tube with a quadrupole mass spectrometer (QMS). This development allows on-line measurements of VOCs at parts per trillion by volume (pptv) levels without any pre-concentrations, and is now used to identify the speciation of VOCs and quantify their mixing ratios in environmental, medical, and food applications [15]. However, simultaneous detection of several VOCs is not achieved due to the use of a quadrupole mass spectrometer for the detection of ions.

Recently, applications of the PTR ionization method to other mass spectrometric detections including ion trap and time-of-flight mass spectrometers (TOFMS) have been reported. The use of ion trap mass spectrometry (ITMS) has the advantage of a high duty cycle. It also has applications of collision-induced dissociation to help diagnose molecular structure of the target species analyzed. For example, a proton transfer reaction-ion trap mass spectrometer (PTR-ITMS) has a potential to distinguish isobaric species (e.g., methacrolein and methylvinyl ketone) [16,17]. The use of TOFMS has an advantage of high mass resolution, leading to explicit identification of the compounds of interest. Proton transfer reaction-time-of-flight mass spectrometer (PTR-TOFMS) instruments with a high mass resolution ($m/\Delta m > 1000$) have been reported, being coupled with radioactive and hollow cathode ion sources [18–20]. Practically, separation of isobaric compounds would be easier with PTR-TOFMS than with PTR-QMS. For example, formic acid (46.0055 amu) and ethanol (46.0419 amu) can be distinguished by PTR-TOFMS [20]. However, the sensitivity of this discharge-based instrument was far less than that of current PTR-QMS instruments. Also, a large amount of NO^+ and O_2^+ ions were produced, likely due to the back-diffusion of air from the drift tube to the hollow cathode ion source [20]. Since the existence of NO^+ and O_2^+ ions makes interpretation of PTR mass spectra more complicated by producing unfavorable ions in the reaction with VOCs, the formation of NO^+ and O_2^+ ions should be suppressed both in the ion source and the drift tube.

We have developed a PTR-TOFMS instrument for simultaneous and real-time detection of VOCs that play important roles in the formation of ozone and secondary organic aerosols (SOA) in air. These species include unsaturated (alkene, diene), oxygenated (aldehyde, ketone, alcohol), and aromatic hydrocarbons. Our PTR-TOFMS instrument is a combination of a custom-built ion source/drift tube and an orthogonal time-of-flight mass spectrometer. The hollow cathode discharge ion source was designed to be coupled with an ion drift tube operated at a pressure of ~5 Torr, which is higher than that of the current PTR-QMS and PTR-TOFMS instruments using a hollow cathode discharge ion source. This has a potential advantage to enhance sensitivity, because a larger amount of sample gases can be introduced into the drift tube. We report here the design and characteristics of our PTR-TOFMS system, and demonstrate its overall performance.

2. Instrumental description

The National Institute for Environmental Studies (NIES) PTR-TOFMS is a custom designed and built instrument, and has been characterized by a number of laboratory experiments. A schematic diagram of the instrument is shown in Fig. 1. It consists of four components: (1) an ion source, (2) a drift tube, (3) an ion transfer chamber, and (4) a time-of-flight mass spectrometer. Air samples are delivered to the instrument by means of 1/8-in. PFA-Teflon tubing with a residence time of less than 10 s. The sample inlet is pressure-controlled by means of a back-pressure controller, but is not temperature-controlled. No particle filter is placed at the inlet to avoid artifact from organics deposited on the filter. The instrument is relatively compact in size, and the overall dimension excluding electronics is 800 mm (W) × 500 mm (D) × 800 mm (H).

In the ion source reagent ions are generated from water vapor introduced as a reagent gas by either radioactive or discharge ion sources. The drift tube is a region where proton transfer reaction occurs from reagent ions to sampled VOCs. In the drift tube, gas phase samples are introduced at the top of it, and ion–molecule reactions between hydronium ions and VOCs take place. Each VOC sampled is then ionized to be $VOC{\cdot}H^+$, as expressed in the following Eq. (1):

$$VOC + H_3O^+ \rightarrow VOC{\cdot}H^+ + H_2O \quad (1)$$

The ion transfer chamber is an interface of the drift tube to a TOFMS. The protonated ions outgoing from the drift cell are extracted, and then directed to a pulse extraction region through

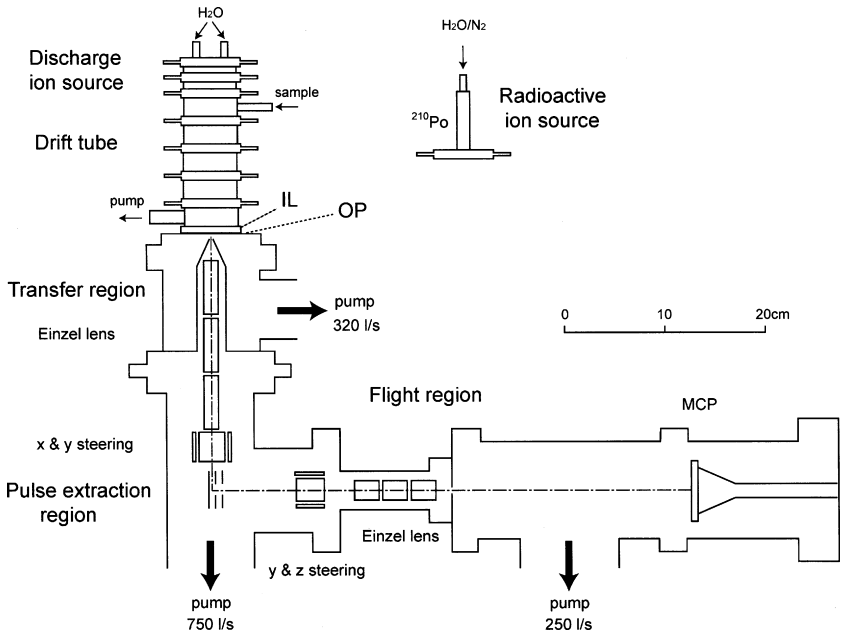

Fig. 1. Schematic diagram of the NIES PTR-TOFMS installment. A discharge ion source, a drift tube, an ion transfer region, a pulse extraction region, and a flight region are illustrated. IL, inlet lens; OP, orifice plate; MCP, multi-channel plate.

an einzel lens. The ions are perpendicularly tilted, and directed to an ion detector by pulsed high voltages applied to the pulser. The mass-to-charge ratios of the ions are determined from flight time measured in the TOFMS. Characterization experiments are described in detail in the following sections.

2.1. Ion source and drift tube

We use both radioactive and discharge ion sources to better characterize our PTR-TOFMS instrument developed in the present work. The radioactive source was used as the reference for the discharge source since it acts as a clean ionizer compared to the discharge source. The radioactive source used is a commercially available linear source with Polonium-210 (370 MBq, P-2021, NRD, New York, USA). For a radioactive source water used as a reagent gas for PTR ionization was obtained by bubbling ultra-high pure N_2 into distilled water (Wako Chemicals, Osaka, Japan), and was introduced into the ion source located at the top of the drift tube. Direct introduction of water vapor, as made with a discharge source, did not work well, while reasons are not clear.

The discharge source was designed and built by our laboratory, and has mainly been used for the present experiments [21,22]. Water used as a reagent gas for PTR ionization is taken from the vapor over distilled water (Wako Chemicals, Osaka, Japan), and was introduced into the ion source at two 1/4-in. inlet ports symmetrically located at the top plate of the ion source. The discharge source region consists of three plates insulated by thin static dissipative Teflon rings (Semitron ESD500, Nippon Polypenco, Tokyo, Japan). The discharge occurs when the voltage at the top electrode is in the range of 3–5 kV. It mainly takes place in the narrow space between the first and the second electrodes, and then expands into the relatively wide area between the second and the third electrodes through a capillary (1 mm i.d., and 12 mm long). Since the drift voltage applied to third plate is 2–4 kV, the field strength (*E*/*N*) of the drift tube ranges from 100 to 160 Td. The ion source is designed to allow high pressure in the drift tube without increasing the back-diffusion of sample air to the ion source, and thus to minimize production of artifact ions NO^+ and $O_2{}^+$. Enhancement of the pressure of the drift tube contributes to increase the amount of sample gases introduced, and thus to achieve high sensitivity.

The design of the ion drift tube and the inlet region to the mass spectrometer in our system is similar to that described by Hanson et al. [23]. The ion drift tube mainly consists of four stainless steel electrodes separated by static dissipative Teflon cylinders. Sample air is introduced at the upstream of the drift tube, which is pumped out through an exhaust port downstream of the drift tube by a diaphragm pump (MD-4, Vacuubrand, Wertheim, Germany). Typical pressure in the drift cell is ~5 Torr. The inlet region to the mass spectrometer consists of two plates, an inlet lens (IL) and an orifice plate (OP). The IL is 3 mm thick and has a 5 mm i.d. hole at the center. The OP is combined with a 50 μm thick and 400 μm i.d. aperture disk of stainless steel (Lenox Laser, Glen Arm, MD, USA). The voltages applied for both plates can be adjusted to reduce highly clustered ions and hence to maximize the relative intensity of H_3O^+ ions. More details on the discharge source are described in our previous paper [21].

Fig. 2 shows distributions of the hydronium ions and its cluster ions as a function of the *E*/*N* ratio in the drift tube. The *E*/*N* ratio acts as an indicator of the collision energy of the ion–molecule reactions in the drift cell. In this experiment, the ion drift tube pressure was kept constant at 5 Torr and the electric field was varied with sample air under relatively dry conditions (absolute humidity of ~0.2%). The high *E*/*N* ratios result in

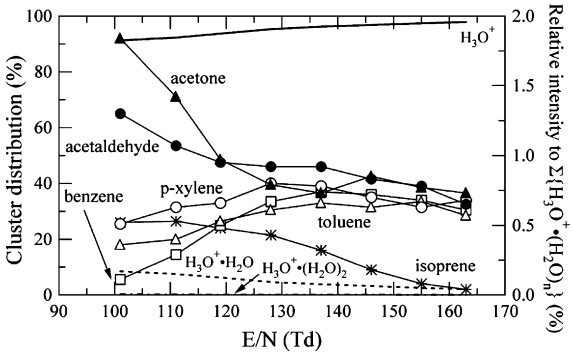

Fig. 2. Dependence of the $H_3O^+\cdot(H_2O)_n$ ($n=0$–2) cluster ion distributions on the *E*/*N* ratio in the drift tube (left axis). Also shown is the dependence of the protonated ions (right axis) for acetaldehyde, acetone, isoprene, benzene, toluene, and *p*-xylene. The drift tube pressure was 5 Torr and the E inlet was kept at 400 V/cm. The sample air containing VOCs was introduced into the instrument under relatively dry condition (absolute humidity of ~0.2%).

enhancement of H_3O^+, and in suppression of its cluster ions (i.e., $H_3O^+\cdot H_2O$ and $H_3O^+\cdot(H_2O)_2$). The H_3O^+ ions dominate more than 90% of the total hydronium ions above 100 Td, and reach as much as 98% at 160 Td. In contrast, $H_3O^+\cdot H_2O$ ions gradually decrease from 8% (100 Td) to 2% (160 Td). The $H_3O\cdot(H_2O)_2$ ions are only less than 0.2% in the range of 100–160 Td. These results suggest that high *E*/*N* values promote the dissociation of water from hydronium ions in the drift tube; similar cluster dissociation might take place in other parts of the instrument (e.g., the exit of the drift tube). The overall signal of H_3O^+ increased from 5×10^5 to 7×10^5 counts with increasing *E*/*N* value from 100 to 160 Td by 1-min integration at a repetition rate of 10 kHz. Although this provides an upper-limit estimate of the H_3O^+ counts in the drift tube, the actual amount of H_3O^+ ions in the drift tube was not exactly known, as discussed below in relation with Fig. 3.

The ion intensities for benzene and toluene substantially increased with increasing *E*/*N* values from 100 to 130 Td, with the maximum around 130–140 Td. The ion intensity for *p*-xylene showed a similar, but more moderate trend. The absolute amount of H_3O^+ ions in the drift tube increased from 100 to 130 Td, and therefore the detection efficiencies for these species would increase. However, the actual amount and distribution of H_3O^+ and its water clusters in the drift tube could not be exactly known with the use of an inlet lens, and the relatively small increase (~30%) in observed H_3O^+ ion signals was probably not a contributing factor to the strong increase in the protonated benzene and toluene. At lower *E*/*N* values substantial amounts of $H_3O^+\cdot H_2O$ ions were observed. While benzene and toluene do not react with $H_3O^+\cdot H_2O$ ions, *p*-xylene does, but slowly. Such differences in the reactions of VOCs with water-clustered hydronium ions would contribute to the observed trends for these species. This assumption is also supported by the trend of acetone, which undergoes fast reactions with $H_3O^+\cdot H_2O$ ions and showed enhanced intensity at lower *E*/*N* values.

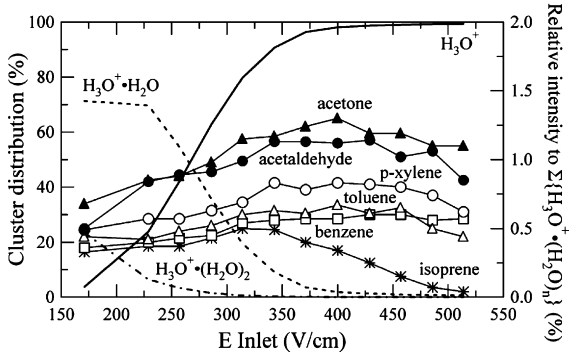

Fig. 3. Dependence of $H_3O^+\cdot(H_2O)_n$ ($n=0$–2) cluster ion distribution on the electric field applied between an inlet lens and an orifice plate (left axis). Also shown is the dependence of the protonated ions (right axis) for acetaldehyde, acetone, isoprene, benzene, toluene, and *p*-xylene. The drift tube pressure and voltage are 5 Torr and 200 V/cm, respectively, resulting in the *E*/*N* value of 135 Td.

The ion intensity for isoprene drastically decreases with the increase in *E*/*N* values from 100 to 160 Td, implying that fragmentation reactions take place with isoprene more effectively. In fact, the ion intensity at 29 amu and 41 amu increases as the decrease in the ion intensity of protonated isoprene (69 amu). This is reasonably explained by the assumption that the 29 amu and 41 amu are $C_2H_5^+$ and $C_3H_5^+$, respectively, produced by the fragmentation of isoprene. The reaction of isoprene with $H_3O^+\cdot H_2O$ might also contribute to the relative increase of protonated isoprene at lower *E*/*N* values. We typically made the following experiments at values in the range of 130–140 Td, which are in good agreement with previous studies [15].

Fig. 3 shows distributions of the hydronium ions and its cluster ions as a function of electric field (*E* inlet) between an inlet lens and an orifice plate. The inlet lens and the orifice plate are often used to focus the ion beam into the transfer region and to reduce the water cluster ion counts. The resulting effect is sometimes confusing with respect to the PTR conditions in the drift tube (i.e., the amount and distribution of hydronium ions and cluster ions). Note that the signals displayed here were not exactly those for the drift tube, where PTR occurs, but rather the overall ion counts detected by the TOFMS. At low electric field, substantial amounts of $H_3O^+\cdot H_2O$ and $H_3O^+\cdot(H_2O)_2$ ions are detected. The $H_3O^+\cdot H_2O$ ions are predominant from 175 to 275 V/cm, showing as much as 70% of the total hydronium ions. However, H_3O^+ ions are predominant at electric field higher than 275 V/cm, and they are more than 90% in the range of 350–500 V/cm. This suggests that cluster distributions of the hydronium ions are largely affected by the electric field at the exit of the drift cell, and that clusterization of the hydronium ions also happen when the ions are ejected from a small exit orifice. The high electric field at the exit of the drift cell is effective to maximize the H_3O^+ intensity by suppressing clustering of the hydronium ions.

The signals of the protonated ions for acetaldehyde, acetone, isoprene, benzene, toluene, and *p*-xylene show moderately increasing trend with the increase in the electric field. These features are in close agreement with those in previous papers [23]. The fact that isoprene shows large dependence on *E* inlet values, suggest that it readily undergoes fragmentation by the increase in collisional energy above 350 V/cm. Although the ion intensity of protonated isoprene starts decreases, we typically set the electric field in the range 350–400 V/cm.

2.2. Time-of-flight mass spectrometer

We use an orthogonal TOFMS for the detection of ions. Our TOFMS consists of an ion transfer region, a pulse extraction region, and a field-free flight region with a multi-channel plate (MCP) ion detector. For the transfer chamber, the pulse extraction region, and the flight tube, turbo-molecular pumps (Varian, Palo Alto, CA, USA) with a pumping speed of 320, 750, 250 l/s, respectively, are deployed, being backed up by two dry scroll pumps (Anest Iwata, ISP-250, Yokohama, Japan). This combination results in pressures of 10^{-4}, 10^{-6}, and 10^{-7} Torr in the transfer chamber, the pulse extraction region, and the flight tube, respectively.

The transfer region acts as an interface between the drift tube and the TOFMS. It is important to minimize the loss of the ions in the ion transfer region to enhance the detection sensitivity, and hence the transfer region is designed to minimize the ion loss by differentially pumping with a conical skimmer (∼2 mm i.d.). Fig. 4 shows ion signals detected as a function of a distance between the drift cell exit orifice and the entrance of the skimmer in the ion transfer region. Not only internal diameter and angle of the skimmer, but the distance is optimized to enhance overall ion intensity detected by the TOFMS. The observed ion intensity of the H_3O^+ ions and $H_3O^+{\cdot}H_2O$ ions has clear dependence on the orifice-skimmer distance with the maximum intensity at 12 mm. The ions are then focused and transported by means of an einzel lens, a set of three cylindrical lenses, toward the pulse extraction module. The pulser is composed of three electrodes, to two of which high voltages are applied using transistor switches (HTS-81, Behlke, Kronberg, Germany). The rise-time of the 5-kV pulse voltage applied to the first electrode of the pulser, defined as the time for the pulse to rise from 10% to 90% of the maximum, was estimated to be 70 ns. This short rise-time is achieved by the use of relatively small resistance obtained by combining six resistors in parallel. The pulse voltage was then kept during 1 μs when the transistor switch was turned on. At 5 kV the fluctuations were in the range of ±0.1 kV (±2σ). The overall resistance used between the first electrode and the ground is 70.5 kΩ, resulting in a heat value of 0.82 mJ per pulse. Since the overall power consumption is substantially reduced, we apply the 5 kV pulse voltage at a frequency of 10 kHz to the pulser. A pulse voltage of 4.5 kV is applied to the second electrode with another set of resistance (70.5 kΩ). A two-dimensional steerer and an einzel lens are used to modify the ion beam direction and to prevent divergence of the beam. We use a 50 cm long single-path flight tube to minimize possible loss of the ions during transport to the detector, while excellent mass resolution is not achieved. The ions are detected with a dual multi-channel plate (MCP, TOF-2003, Burle, Lancaster, PA, USA) ion detector. The ion signals are transferred to a time-to-digital converter (TDC, P7887, Fast Com Tec, Oberhaching, Germany) with 2 ns time bins, where the ion signals are discriminated, counted, and integrated during 1–5 min at a repetition rate of 10 kHz. The mass number is calibrated against the reference mass spectra obtained in the discharge of noble gases (e.g., Kr and Xe). The full width at half maximum (FWHM) at current conditions is 0.35, 0.56, and 0.60 at 19, 59, and 107 amu, respectively.

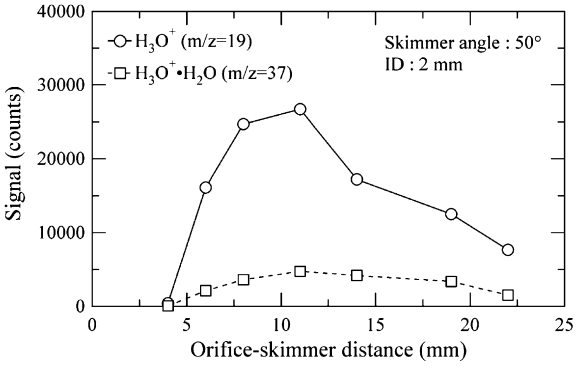

Fig. 4. The signals of H_3O^+ ($m/z = 19$) and $H_3O^+{\cdot}H_2O$ ($m/z = 37$) ions as a function of distance between an exit orifice of the drift tube and a skimmer of the ion transfer region.

3. Results and discussion

3.1. PTR mass spectra with a radioactive ion source

Fig. 5 shows PTR mass spectra of zero-air and seven VOCs obtained with a radioactive ion source (^{210}Po, 370 MBq). Water vapor was introduced by bubbling liquid water in the reservoir with ultra-pure N_2 from a gas cylinder. The optimized pressure and the E/N ratio of the drift tube were 7 Torr and 123 Td, respec-

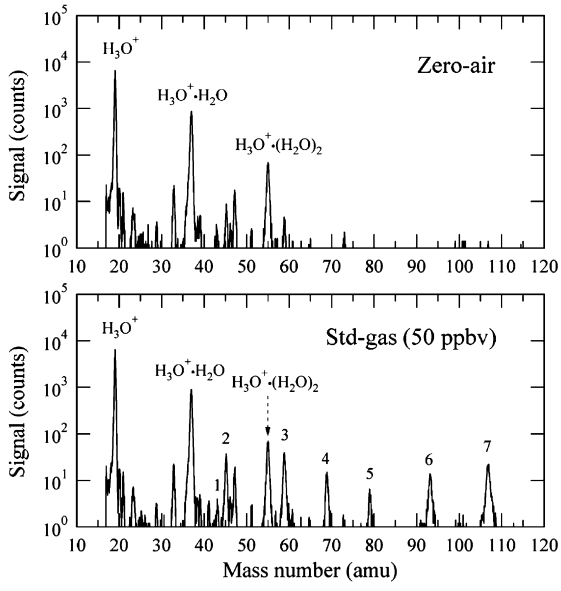

Fig. 5. PTR mass spectra (upper panel) of zero-air supplied by pressurized ultra-high purity air, and (lower panel) of seven VOCs (propene, acetaldehyde, acetone, isoprene, benzene, toluene, and *p*-xylene) at 50 ppbv mixing ratios provided by dilution of the standard gases (5 ppmv) with zero-air, obtained with a radioactive ion source (^{210}Po source, 370 MBq). Pressure and the E/N of the drift tube were 7 Torr and 123 Td, respectively. The data were integrated during 1 min at a repetition rate of 10 kHz. The index numbers are: 1, propene, 43 amu; 2, acetaldehyde, 45 amu; 3, acetone, 59 amu; 4, isoprene, 69 amu; 5, benzene, 79 amu; 6, toluene, 93 amu; and 7, *p*-xylene, 107 amu.

tively. The data were integrated during 1 min at a repetition rate of 10 kHz. The use of a radioactive source makes it possible for us to increase the drift tube pressure up to 7 Torr, where the partial pressure of H_2O/N_2 and the sample air is 2 and 5 Torr, respectively. The mass spectra of zero-air supplied by pressurized cylinders of ultra-high purity air show a prominent peak of H_3O^+ (19 amu) and a small peak of $H_3O^+{\cdot}H_2O$ (37 amu). The peak of $H_3O^+{\cdot}(H_2O)_2$ is identified at 55 amu, though it is much smaller than other two peaks. The other minor peak observed at 21 amu is assigned to be $H_2{}^{18}O^+$. The peaks at 33 and 47 amu, attributed to $CH_3OH{\cdot}H^+$ and $C_2H_5OH{\cdot}H^+$, respectively, were probably due to impurities of methanol, and ethanol and/or formic acid. There are also some background signals of acetaldehyde and acetone at 45 and 59 amu, respectively.

The mass spectra are examined for seven VOCs. The VOCs gas standard containing propene (C_3H_6), acetaldehyde (CH_3CHO), acetone ($CH_3C(O)CH_3$), isoprene (C_5H_8), benzene (C_6H_6), toluene ($C_6H_5(CH_3)$), and *p*-xylene ($C_6H_4(CH_3)_2$) is gravimetrically prepared in a aluminum gas cylinder balanced in nitrogen (5 ppmv, Japan Fine Products, Kawasaki, Japan). The stream of the standard gas is dynamically diluted with dry zero-air provided by either a zero-air generator or ultra-high purity air cylinders (99.9999%, Japan Fine Products, Kawasaki, Japan) to be parts per billion by volume (ppbv) levels. The measurements made at the VOC mixing ratios of 50 ppbv show the peaks of H_3O^+ (19 amu), $H_3O{\cdot}H_2O$ (37 amu), and $H_3O{\cdot}(H_2O)_2$ (55 amu). In addition to these three peaks originated from the reagent ions, six apparent peaks at 45, 59, 69, 79, 93, and 107 amu and a very small peak at 43 amu are observed. These peaks correspond to protonated VOCs: acetaldehyde, acetone, isoprene, benzene, toluene, *p*-xylene, and propene, respectively. The results reveal that the instrument background with a ^{210}Po radioactive source is relatively small, and emerging artifact signals including NO^+ or $O_2{}^+$ ions were not observed. The fact that either NO^+ or $O_2{}^+$ ions are not observed suggest that the background mass spectra are not affected by the introduction of the sample air. Although detection of propene is not well achieved, other six species are clearly identified at quantification levels.

3.2. PTR mass spectra with a hollow cathode discharge ion source

Fig. 6 shows PTR mass spectra of zero-air and seven VOCs obtained with a discharge ion source. Water vapor was directly introduced from the headspace of liquid water in the reservoir without any bubbling. The optimized pressure and the *E*/*N* ratio of the drift tube were 5 Torr and 135 Td, as the discharge is not stable enough at the pressure greater than 5 Torr. The absolute abundance of the reagent ions is more intense than that obtained with the radioactive source. It is estimated to be approximately one order of magnitude stronger. The relative abundance of $H_3O^+{\cdot}H_2O$ and $H_3O^+{\cdot}(H_2O)_2$ ions in reference to H_3O^+ was suppressed at much smaller levels than with the radioactive source, probably because more water vapor was introduced into the ion source. The efficiency of the proton transfer reaction from hydronium ions to VOCs became approximately 3 times higher for all seven compounds. Note that peaks of artifact signals of NO^+ (30 amu) and $O_2{}^+$ (32 amu) were identified, because these ions can compete and interfere with hydronium ions in the PTR ionization of VOCs [24–27]. Several other peaks are also significantly identified in the background mass spectra, indicating that the discharge source was dirtier than the radioactive source and provided a higher instrument background. Detailed peak assignments were described previously [21]. However, the levels of these background ions were smaller compared to previous studies reporting a PTR-TOFMS with a hollow cathode discharge source [20], and subtraction of the background mass spectrum from the sample mass spectrum cancels potential interferences from these background ions for the detection of trace amount of VOCs, as demonstrated by Inomata et al. [21].

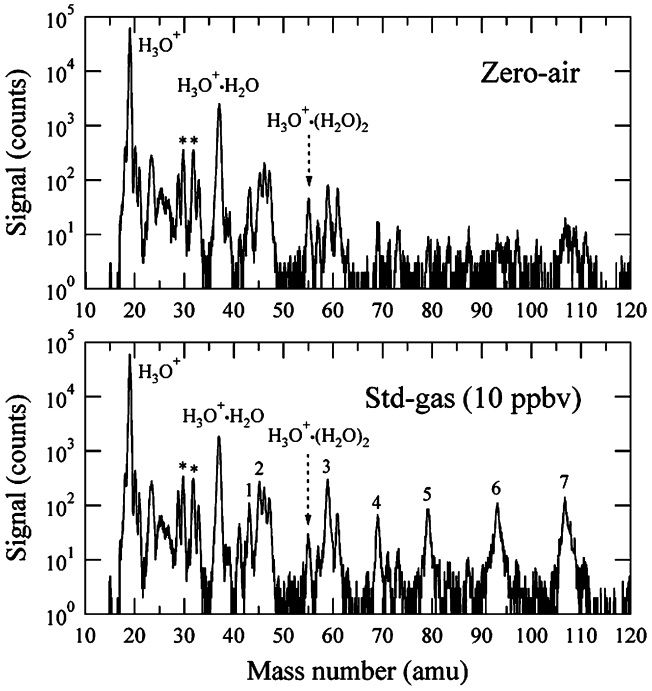

Fig. 6. Same as Fig. 5, but obtained with a hollow cathode discharge ion source. The mixing ratios of VOCs are 10 ppbv. Pressure and the *E*/*N* of the drift tube were 5 Torr and 135 Td, respectively. The data were integrated during 1 min at a repetition rate of 10 kHz. Two artifact signals of NO^+ and $O_2{}^+$ are indicated with asterisks (*).

Measurements of the standard gases show seven apparent peaks at 43, 45, 59, 69, 79, 93, and 107 amu, corresponding to protonated VOCs: propene, acetaldehyde, acetone, isoprene, benzene, toluene, and *p*-xylene, respectively. This demonstrates that all the seven VOCs including alkenes, carbonyls, and aromatics are simultaneously detected as the form of protonated ions at ppbv levels with the discharge source by our PTR-TOFMS instrument. The background signals observed do not change except small consumption of NO^+ and $O_2{}^+$ ions, between the background and the sample mass spectra, indicating that these influence can be canceled by frequently performing background measurements during the course of measurements of sample air, even if the discharge source provides higher instrument background than the radioactive source does.

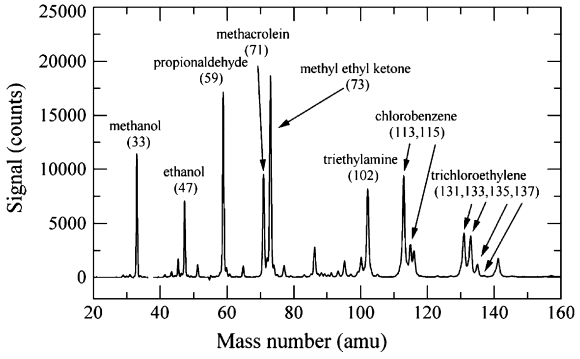

Fig. 7. PTR mass spectra of several alcohols, ketones, amines, and halogenated carbons at ppbv levels with a hollow cathode discharge source. Pressure and the *E/N* of the drift tube were 5 Torr and 120 Td, respectively. The spectra shown are sample minus the background.

3.3. Performance and demonstration

We explored possibilities of our PTR-TOFMS instrument to detect other compounds of atmospheric or environmental interest. Fig. 7 shows mass spectra of the samples containing several alcohols (methanol, ethanol), carbonyls (propionaldehyde, methacrolein, methylethylketone), amines (triethylamine), and halocarbons (chlorobenzene, trichloroethylene) with a hollow cathode discharge source. The samples were prepared by static dilution of vaporized reagent liquid with dry zero-air. The mixing ratios of each species were at sub-part per million by volume (ppmv) levels. All the eight species tested are successfully detected as the protonated ions. For chlorobenzene and trichloroethylene, the signals are split into two (113 and 115 amu) and four (131, 133, 135, and 137 amu) peaks, respectively. This originates from the existence of chlorine isotopes (^{35}C1 and ^{37}C1), of which natural abundance is estimated as 3:1.

Fig. 8 shows response of the ion signals of protonated VOCs in the range of 0–100 ppbv levels observed by our PTR-TOFMS instrument. Samples of VOCs at ppbv-levels were prepared by dynamic dilution of gas standards by dry zero-air. The least square fits clearly indicate excellent linearity ($R^2 > 0.99$) and negligible intercepts for acetaldehyde, acetone, isoprene, benzene, toluene, and *p*-xylene. For propene, however, a poor linear response and a small intercept were observed, probably because of a lower sensitivity than for the other six compounds and of fragments from other compounds such as acetone (data not shown).

The detection sensitivities of our PTR-TOFMS instrument to the seven species were calculated based on the linear responses discussed above, and were normalized against H_3O^+ signals at 1×10^6 counts (Table 1). With an integration time of 1 min, the normalized sensitivities were 13, 174, 237, 102, 34, 111, and 184 ncounts/ppbv for propene, acetaldehyde, acetone, isoprene, benzene, toluene, and *p*-xylene, respectively. In order to compare our sensitivities to values obtained previously with PTR-QMS, conversion factors (c.f.) were applied to convert normalized counts/ppbv into normalized counts per second (cps)/ppbv (Eq. (2)):

$$\left[\frac{\text{ncps}}{\text{ppbv}}\right] = \text{c.f.} \times \left[\frac{\text{ncounts}}{\text{ppbv}}\right] \quad (2)$$

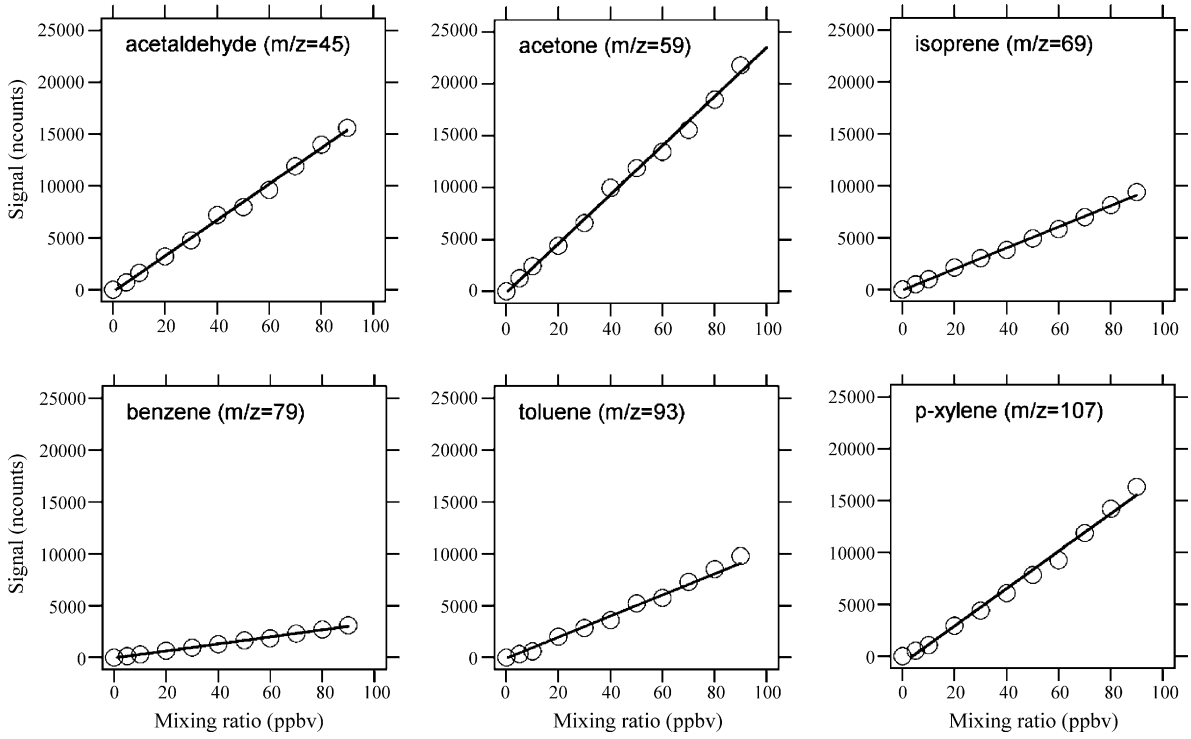

Fig. 8. Instrument responses to VOCs in the range of 0–100 ppbv. Measurements were integrated during 1 min at a repetition rate of 10 kHz at a pressure of 5 Torr; the *E/N* of the drift tube was 135 Td. Signals on the vertical axis are peak area basis of sample minus background measurements, and are normalized to those with H_3O^+ signals at 1×10^6 counts.

Table 1
Sensitivities of the NIES PTR-TOFMS instrument to seven VOCs

Species (detected mass)	Normalized sensitivity[a] (ncounts/ppbv)	Conversion factor $\sqrt{19/M}$	Normalized sensitivity[a] (ncps/ppbv)	Hanson et al. [23]	de Gouw et al. [28], Warneke et al. [29]	Whyche et al. [30]	Ennis et al. [20]
Propene (43)	13 ± 3	0.665	9 ± 2	–	16	–	–
Acetaldehyde (45)	174 ± 9	0.650	113 ± 6	90–115	27	50	–
Acetone (59)	237 ± 11	0.567	134 ± 6	240	64	51	28
Isoprene (69)	102 ± 5	0.525	54 ± 3	120	32	–	–
Benzene (79)	34 ± 2	0.490	17 ± 1	–	34	–	–
Toluene (93)	111 ± 7	0.452	50 ± 3	–	45	26	4
p-Xylene (107)	184 ± 13	0.421	77 ± 6	–	19	–	–

[a] Sensitivities are normalized to those with H_3O^+ signals at 1×10^6 counts, and error bars are 95% confidence levels by *t*-test. ncounts/ppbv, normalized counts per parts per billion by volume; ncps/ppbv, normalized counts per second per parts per billion by volume.

The conversion factors were calculated with reference to the ion intensity of H_3O^+ (19 amu), and are mass-number dependent (i.e., the factor decreases with increasing mass number), taking the mass dependency of the duty cycle in TOFMS into account [21].

This eventually provides conservative estimates, even though uncertainties of the conversion factors are taken into account. The normalized sensitivities per second for propene, acetaldehyde, acetone, isoprene, benzene, toluene, and *p*-xylene were determined to be 9, 113, 134, 54, 17, 50, and 77 ncps/ppbv, respectively, and could be compared to previously reported values obtained with PTR-QMS and PTR-TOFMS [20,23,28–30].

Our sensitivities for acetaldehyde, acetone, and isoprene are comparable to the values reported by Hanson at al. [23] and are larger than those obtained in other studies [20,28–30]. This is likely due to the relatively high drift tube pressure attained in our instrument, as enhancement of the drift tube pressure greatly improves sensitivity in conventional PTR-QMS measurements [23]. The fact that isoprene showed a relatively smaller sensitivity, may be because our system was operated at a higher *E*/*N* value (135 Td) than Hanson et al. (110 Td), allowing more fragmentation. For aromatics, the sensitivities in the present work may not be compared with those from Hanson et al. [23], but can be compared with PTR-QMS results reported by de Gouw et al. [28] and Warneke et al. [29]. The sensitivity values for toluene and *p*-xylene are comparable to or even higher than those reported by de Gouw et al. [28] and Warneke et al. [29], but that of benzene is significantly smaller, likely because of the unknown cluster distribution in the drift tube. Comparisons with the latest performance values of other PTR-TOFMS instruments [20,30] suggest that the sensitivities obtained in this work are approximately double those reported by Whyche et al. [30]. The large difference with the values reported by Ennis et al. [20] who deployed a discharge ion source, was likely due to the difference in pressure in the drift tube.

We calculated the detection limits for the seven VOC species, based on signals (peak height) and noise (fluctuation of background level), hence signal-to-noise ratios (S/N) in the sample—i.e., the background mass spectrum. The background and noise levels were found to depend slightly on the mass number. We observed more background signals in the lower mass region and less in the higher mass region, due to instrument background signals produced by the discharge source (Fig. 6). The background ranged from less than 1 to 4 counts and the noise (2σ fluctuations of the background level) around the target peaks typically ranged from 2 to 5 counts (both as raw signals). The current detection limits at S/N = 2 were determined to be 2282, 393, 290, 778, 540, 485, and 362 pptv for propene, acetaldehyde, acetone, isoprene, benzene, toluene, and *p*-xylene, respectively, for a 1-min integration time. Propene shows the highest detection limit due to its low sensitivity. The detection limit for isoprene is not as good as for other species, likely because of decomposing fragmentation, which possibly takes place with our current settings. Although acetaldehyde and acetone had higher peak heights than aromatics, the noise levels for mass numbers between 40 and 60 amu were also higher, limiting the detection of acetaldehyde and acetone.

Fig. 9 shows cluster distribution and the dependence of the sensitivity for seven VOCs on water vapor content in sample air. The signals are normalized against H_3O^+ signals. The relative abundance of $H_3O^+ \cdot H_2O$ ions gradually increased with the

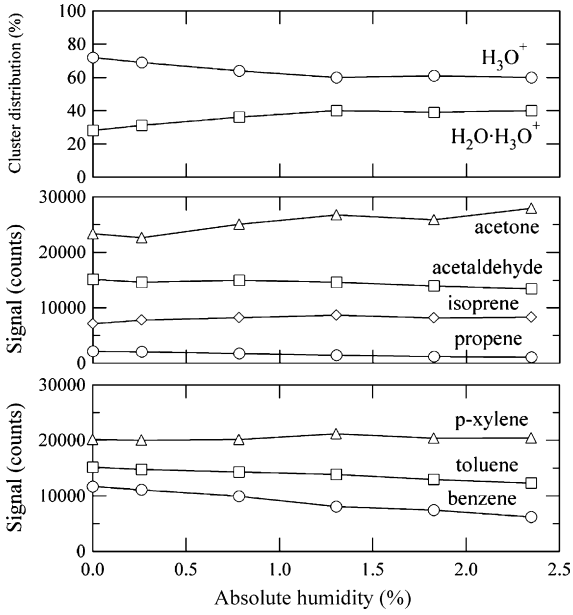

Fig. 9. Cluster distribution (top panel) and sensitivity dependence for several VOC species (middle and bottom panel) on absolute humidity (v/v) in sample air. The *E*/*N* ratio is 135 Td, and the drift tube pressure is 5 Torr. The room temperature is 22 °C. The signals are normalized to those with H_3O^+ signals at 1×10^6 counts.

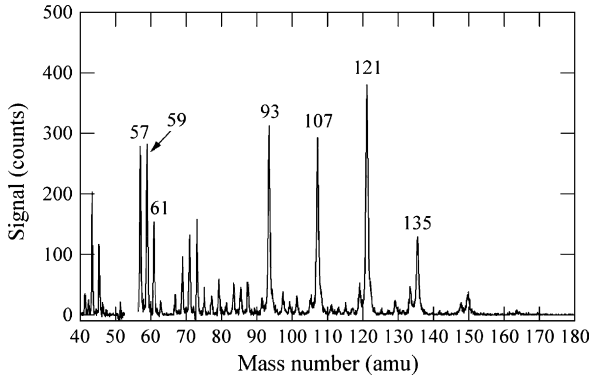

Fig. 10. An example of PTR mass spectra observed in car exhaust plume. The background mass spectrum is subtracted from that of the sample. The spectrum was integrated during 1 min at a repetition rate of 10 kHz. The ion signals at 55 amu ($H_3O^+ \cdot (H_2O)_2$) are masked.

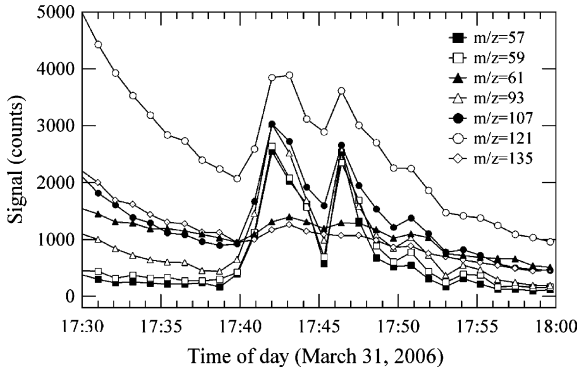

Fig. 11. Temporal variations of the ion signals for the major seven mass numbers observed in car exhaust plume. The ion signals plotted are peak area for minutely data.

increase in absolute humidity in sample air. The tendency of the dependence differs for each species. The ion signals of protonated benzene and toluene decrease with the increase in the absolute humidity. In contrast, the signals of protonated acetone increase with the increase in the absolute humidity. Propene, acetaldehyde, isoprene, and *p*-xylene show almost constant trend along with the absolute humidity. This feature is in close agreement with those reported in previous papers [23,31]. Different behaviors in these VOC signals with humidity are probably due to differences in reactions with water-clustered hydronium ions, as there are no PTR reactions of benzene and toluene with $H_3O^+ \cdot H_2O$ and $H_3O^+ \cdot (H_2O)_2$, but with acetone such reactions are very efficient [31].

Fig. 10 shows an example of PTR mass spectra observed during measurements of exhaust gas from vehicle using gasoline. Plumes from car exhaust were directly sampled by means of 1/4-in. Teflon tubing for subsequent detection by the PTR-TOFMS instrument. Mainly observed were peaks at the mass numbers 57, 59, 61, 93, 107, 121, and 135 amu. It should be noted that one can not explicitly identify the VOCs only by interpretation of PTR mass spectra, since compounds that have the same mass number including isobaric compounds and structural isomers appear at the same mass-to-charge ratios. Also the PTR ionization sometimes causes fragmentation for relatively fragile species including alkenes, terpenes, and multifunctional organics [32]. Therefore, accurate identification and quantification of VOCs by PTR-MS in unknown samples needs auxiliary analysis with well-established techniques, conventionally, for example, gas chromatography–mass spectrometry methods [28,33]. Therefore, although explicit identification was not made in this work, possible peak assignment suggests that butene (C_4H_8)/2-methyl-1-propene (C_4H_8) (57 amu), acetone (C_3H_6O)/propionaldehyde (C_3H_6O) (59 amu), acetic acid ($C_2H_4O_2$)/l-propanol (C_3H_8O)/isopropanol (C_3H_8O) (61 amu), toluene (C_7H_8) (93 amu), xylenes (C_8H_{10}) (107 amu), trimethylbenzene (C_9H_{12}) (121 amu), and tetramethylbenzene ($C_{10}H_{14}$) (135 amu). These mass peaks were detected in the PTR-QMS measurements of diesel engine exhaust, suggesting that benzene and toluene are of pyrogenic origin [34].

Fig. 11 depicts temporal variations of the ion signals observed in car exhaust. Minutely data are plotted for major seven mass numbers identified (i.e., 57, 59, 61, 93, 107, 121, 135 amu). The instrument is able to follow quickly changing mixing ratios at

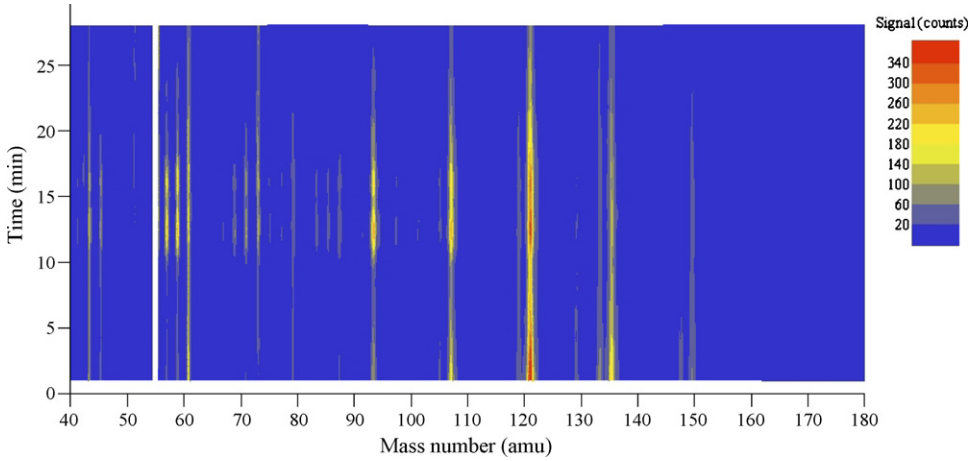

Fig. 12. Ion intensities of VOCs from car exhaust as a function of time and the mass number from 40 to 180 amu. The ion signals at 55 amu ($H_3O^+ \cdot (H_2O)_2$) are masked. Minutely data are plotted.

ppmv levels of several VOCs from the emission source in real-time. Several species including those with mass numbers of 57, 59, 93, 107, and 121 amu show large temporal variation on short time scales even on the order of minutes, depending on the status of the engine (e.g., idling or accelerating). In contrast, the changes in the mass signals at 61 and 135 amu were rather smooth, implying that behavior of the VOCs emitted from the car exhaust depends on speciation, or that these sticky compounds are influenced by memory effects in the gas inlet and Teflon plumbing.

Fig. 12 illustrates the ion intensities of VOCs from car exhaust as a function of the mass number and measurement time. Large ion intensity is found at the mass numbers of 57, 59, 61, 93, 107, 121, and 135 amu. The mass number at 121, very likely that of protonated trimethylbenzene, reveals the most abundant intensity among all peaks identified. Several other peaks are also identified at the mass numbers of 43, 45, 69, 71, 73, 79, 83, 85, 87, 119, 133, and 149 amu. Although these peaks are all in small amounts, their temporal variations correspond well to those of major seven peaks displayed in Fig. 11. These behaviors highlight two-dimensional views of the variability of VOCs outgoing of the car exhaust, and demonstrate possible applications of PTR-TOFMS in emission studies to characterize VOCs released from the primary sources.

4. Conclusions

A proton transfer reaction-time-of-flight mass spectrometer has been developed for real-time measurements of organic compounds in air. A custom-built hollow cathode discharge source is employed for the ion source to facilitate deployment of the instrument in field studies. These efforts enable us to perform highly time-resolved measurements of VOCs with improved absolute detection limits compared to similar systems.

To summarize the overall performance of the NIES PTR-TOFMS instrument, the system can detect ions as heavy as 30,000 amu with a 10 kHz repetition rate, but we normally record the mass signals in the range of 10–1000 amu. While the mass resolution is ~100, which is not as high as in systems equipped with a reflectron [18–20], the absolute detection sensitivity and hence the detection limit are greatly improved. The duty cycle is ~1%. The absolute H_3O^+ intensity with the discharge source was about one order of magnitude larger than that with the radioactive source. We determined the lower detection limit (S/N = 2) with the discharge source to be in the range of sub-ppbv for acetaldehyde, acetone, isoprene, and aromatic species with 1-min integration time. The stability of the ion source is within 4% for 6 h, but evaluation of the lifetime of the discharge source, and the frequency of the maintenance (cleaning and recovery) needs further experiments. Preliminary experiments suggest that the sensitivity can be significantly recovered by cleaning with alkaline solution, but not with an acidic one.

Future improvements include deployment of a reflectron for high-mass resolution, and improvement of the ion transfer region to minimize the ion loss. Characterization and optimization of the sample inlet conditions in the field are further tasks to be addressed. The PTR-TOFMS instrument can be a powerful technique for studies, in which real-time measurements of several VOCs in air at trace levels are needed. These include characterization of VOCs from emission sources, field observations of short-lived species, and laboratory studies on chemical transformation of VOCs.

Acknowledgements

The authors are grateful to Tomonari Wakabayashi (Kinki University), Haruo Shiromaru (Tokyo Metropolitan University), and Naoaki Saito (AIST) for providing useful information in the initial stage of this study. David R. Hanson (NCAR), Paul S. Monks and Andrew M. Ellis (University of Leicester) are gratefully acknowledged for valuable comments and discussions on PTR-TOFMS instrumentation. We thank technical support from Haruka Sasaki (IERIC) in the instrumentation, and from Miori Ohno (National Institute for Environmental Studies) in software development. Two anonymous reviewers are acknowledged for valuable comments, which helped us to improve the manuscript. This study was financially supported by Environmental Technology Development Fund (FY 2004–2005) of the Ministry of the Environment, and partly by the Steel Industry Foundation for the Advancement of Environmental Protection Technology (FY2005).

References

[1] B.J. Finlayson-Pitts, J.N. Pitts, Chemistry of the Upper and Lower Atmosphere, Academic Press, New York, USA, 2000.
[2] R. Atkinson, Atmos. Environ. 34 (2000) 2063.
[3] A.C. Lewis, N. Carslaw, P.J. Marriott, R.M. Kinghorn, P. Morrison, A.L. Lee, K.D. Bartle, M.J. Pilling, Nature 405 (2000) 778.
[4] A. Guenther, C.N. Hewitt, D. Erickson, R. Fall, C. Geron, T. Graedel, P. Harley, L. Klinger, M. Lerdau, W.A. McKay, T. Pierce, B. Scholes, R. Steinbrecher, R. Tallamraju, J. Taylor, P. Zimmerman, J. Geophys. Res. 100 (1995) 8873.
[5] W.J. Broadgate, P.S. Liss, S.A. Penkett, Geophys. Res. Lett. 24 (1997) 2675.
[6] J. Kesselmeier, P. Ciccioli, U. Kuhn, P. Stefani, T. Biesenthal, S. Rottenberger, A. Wolf, M. Vitullo, R. Valentini, A. Nobre, P. Kabat, M.O. Andreae, Global Biogeochem. Cycles 16 (2002) 1126, doi:10.1029/2001GB001813.
[7] P. Di Carlo, W.H. Brune, M. Martinez, H. Harder, R. Lesher, X.R. Ren, T. Thornberry, M.A. Carroll, V. Young, P.B. Shepson, D. Riemer, E. Apel, C. Campbell, Science 304 (2004) 722.
[8] H. Singh, Y. Chen, A. Staudt, D. Jacob, D. Blake, B. Heikes, J. Snow, Nature 410 (2001) 1078.
[9] R. Holzinger, J. Williams, G. Salisbury, T. Kluepfel, M. de Reus, M. Traub, P.J. Crutzen, J. Lelieveld, Atmos. Chem. Phys. 5 (2005) 39.
[10] T. Karl, T. Jobson, W.C. Kuster, E. Williams, J. Stutz, R. Shetter, S.R. Hall, P. Goldan, F. Fehsenfeld, W. Lindinger, J. Geophys. Res. 108 (2003) 4508, doi:10.1029/2002JD003333.
[11] J.A. de Gouw, A.M. Middlebrook, C. Warneke, P.D. Goldan, W.C. Kuster, J.M. Roberts, F.C. Fehsenfeld, D.R. Worsnop, M.R. Canagaratna, A.A.P. Pszenny, W.C. Keene, M. Marchewka, S.B. Bertman, T.S. Bates, J. Geophys. Res. 110 (2005) D16305, doi:10.1029/2004JD005623.
[12] D. Helmig, J. Chromatogr. A 843 (1999) 129.
[13] A. Hansel, A. Jordan, R. Holzinger, P. Prazeller, W. Vogel, W. Lindinger, Int. J. Mass Spectrom. Ion Processes 149/150 (1995) 609.
[14] W. Lindinger, A. Hansel, A. Jordan, Chem. Soc. Rev. 27 (1998) 347.
[15] W. Lindinger, A. Hansel, A. Jordan, Int. J. Mass Spectrom. Ion Processes 173 (1998) 191.
[16] P. Prazeller, P.T. Palmer, E. Boscaini, T. Jobson, M. Alexander, Rapid Commun. Mass Spectrom. 17 (2003) 1593, doi:10.1002/rcm.l088.

[17] C. Warneke, J.A. de Gouw, E.R. Lovejoy, P.C. Murphy, W.C. Kuster, R. Fall, J. Am. Soc. Mass Spectrom. 16 (2005) 1316, doi:10.1016/j.jasms.2005.03.025.
[18] R.S. Blake, C. Whyte, C.O. Hughes, A.M. Ellis, P.S. Monks, Anal. Chem. 76 (2004) 3841, doi:10.1021/ac0498260.
[19] K.P. Whyche, R.S. Blake, K.A. Willis, P.S. Monks, A.M. Ellis, Rapid Commun. Mass Spectrom. 19 (2005) 3356, doi:10.1002/rcm.2202.
[20] C.J. Ennis, J.C. Reynolds, B.J. Keely, L.J. Carpenter, Int. J. Mass Spectrom. 247 (2005) 72, doi:10.1016/j.ijms.2005.09.008.
[21] S. Inomata, H. Tanimoto, N. Aoki, J. Hirokawa, Y. Sadanaga, Rapid Commun. Mass Spectrom. 20 (2006) 1025.
[22] N. Aoki, S. Inomata, H. Tanimoto, Int. J. Mass Spectrom. 263 (2007) 12, doi:10.1016/j.ijms.2006.11.018.
[23] D. Hanson, J. Greenberg, B.E. Henry, E. Kosciuch, Int. J Mass Spectrom. 223–224 (2003) 507.
[24] N. Schoon, C. Amelynck, L. Vereecken, E. Arijs, Int. J. Mass Spectrom. 229 (2003) 231, doi:10.1016/S1387-3806(03)00343-9.
[25] E. Michel, N. Schoon, C. Amelynck, C. Guimbaud, V. Catoire, E. Arijs, Int. J. Mass Spectrom. 244 (2005) 50, doi:10.1016/j.ijms.2005.04.005.
[26] C. Amelynck, N. Schoon, T. Kuppens, P. Bultinck, E. Arijs, Int. J. Mass Spectrom. 247 (2005) 1, doi:10.1016/j.ijms.2005.08.010.
[27] T. Wang, P. Spanel, D. Smith, Int. J. Mass Spectrom. 239 (2004) 139, doi:10.1016/j.ijms.2004.07.022.
[28] J.A. de Gouw, P.D. Goldan, C. Warneke, W.C. Kuster, J.M. Roberts, M. Marchewka, S.B. Bertman, A.A.P. Pszenny, W.C. Keene, J. Geophys. Res. 108 (2003) 4682, doi:10.1029/2003JD003 863.
[29] C. Warneke, J.A. de Gouw, W.C. Kuster, P.D. Goldan, R. Fall, Environ. Sci. Technol. 37 (2003) 2494.
[30] K.P. Wyche, R.S. Blake, A.M. Ellis, P.S. Monks, T. Brauers, R. Koppmann, E. Apel, Atmos. Chem. Phys. Discuss. 6 (2006) 10247.
[31] C. Warneke, C. van der Veen, S. Luxembourg, J.A. de Gouw, A. Kok, Int. J. Mass Spectrom. 207 (2001) 167.
[32] A. Tani, S. Hayward, C.N. Hewitt, Int. J. Mass Spectrom. 223–224 (2003) 561.
[33] S. Kato, Y. Miyakawa, T. Kaneko, Y. Kajii, Int. J. Mass Spectrom. 235 (2004) 103, doi:10.1016/j.ijms.2004.03.013.
[34] B.T. Jobson, M.L. Alexander, G.D. Maupin, G.G. Muntean, Int. J. Mass Spectrom. 245 (2005) 78, doi:10.1016/j.ijms.2005.05.009.